Development of Magnisio Ferrite Doped Polymer Electrolyte System for Battery Application

Kamlesh Pandey* Markandey Singh, Nidhi Asthana, Mrigank Mauli Dwivedi, and S.L. Agrawal[1]
National centre of Experimental Mineralogy and Petrology, University of Allahabad, Allahabad-211002
[1]Department of Physics, A. P.S. University, Rewa (M.P.)
*kp542831@yahoo.com

Abstract-**Ion transport property of [93PEO-7NH_4SCN]: Mg-Zn Magnisio ferrite electrolyte system have been investigated here with the aim of developing a high performance solid state battery. Wet chemistry route has been adopted to obtain this electrolyte. XRD patterns (Debye-Scherer & Williamson Hall plot calculations) ascertain formation of nanocomposite system. Different ion transport parameters like bulk conductivity, dielectric loss, tangent loss and modulus spectra were studied with the aid of impedance spectroscopic data. Optimum d.c. conductivity has been observed for [93PEO-7NH_4SCN]: 1wt% Mg-Zn ferrite system ($9.0x10^{-5}$ S/cm) and a.c. conductivity of nanocomposite polymer electrolytes seems to follow the universal power law. Battery performance of this electrolyte was tested and OCV of best system is found to be 1.57 Volt.**

KeyWords-Dielectric Relaxation; Magnisio ferrite; Polymer nano composite; polymer salt interaction; PEO, Proton conducting battery.

I. INTRODUCTION

Nanocomposite polymer electrolyte (NCPE) materials are receiving special attention, particularly in the field of solid state ionics owing to their potential applications in advanced ionic devices such as high performance batteries, fuel cell, supercapacitor, sensors, smart window etc. [1-4]. NCPE have several distinct advantages over liquid electrolytes such as good mechanical properties, better thermal stability, corrosionlessness, light weight, flexibility and ease of fabrication / processibility as thin films etc. PEO is one of the most prominent polymer host which has been extremely investigated as polymer electrolyte using alkali salts, plasticizer and inorganic fillers in the recent past [5,6]. The other polymer host poly (vinyl alcohol) [PVA] , poly (vinyl chloride) [PVC], poly (vinylidenefluoride) [PVdF], poly (methyl methacrylate) [PMMA] have been also studied for potential material [7-12]. In spite of the industrial importance and wide application of PEO poly (ethylene oxide), the ions conduction mechanism remains unresolved. The chemical structure of PEO i.e. [$(CH_2\text{-}CH_2\text{-}0)_n$] explain most of the properties of this polymer, a strong solvating character due to high donating character of numerous either oxygen, strong tendency for crystallization correlated to high organization and rigidity of segmental units. As earlier most of workers have been stated experimental work, anion / cation mobility occurs in the amorphous phase and its diffusion occurs through a complex mechanism involving the PEO segmental mobility. For that, crystallization has to be avoided by modifying the pure polymer structure or by adding salt or by one or more plasticizer or filler to inhibit regular packing. Moderate conductivity in amorphous material is then a direct consequence of PEO features where high salvation is counter balanced by the energetic complexation of cations. Equilibrium between different solvated species (free ions, solvent separated ion pairs, ion pairs or high ions aggregation) also has a detrimental effect on cation mobility [13]. The addition of ferrite filler to PEO matrix enhances the polar characteristic of PEO making it electrically more conductive. When PEO is doped with ferrites, it may reside at various sites. It may go substitution on polymer chain at the amorphous or crystalline boundaries and preferentially into amorphous regions of polymer. Furthermore, it is asserted that addition of ferrite creates additional hopping sites for the charge carriers and hence increases in its concentration, increase the conductivity [14, 15].

In view of the above, an innovative approach has been made to use nanosized Mg-Zn ferrite ceramics material as filler in development of PEO-NH_4SCN electrolyte based NCPE and its electrical characterization in the present work. The structural aspect of composite electrolytes has been studied by XRD measurement and the effect of salt or filler in enhancement of a.c. conductivity of NCPE under different conditions. The frequency and temperature dependent behavior of dielectric, modulus spectra and a.c. conductivity have been investigated.

II. EXPERIMENTAL:

The Mg-Zn ferrite powder was synthesized by the standard sol-gel technique. Different nitrates were (like Mg (NO3)2.6H2O, Fe (NO3).9H2O and Zn (NO3)2.6H2O AR grade) have been used as the starting chemicals to obtain the Fe3+, Mg2+, Zn2+ & Fe2+ ions in aqueous solution. These nitrates were dissolved in double distilled water/ethanol mixture. The pH of solution was fixed within 2-3 range. The sol allowed to gel at 50oC. The gel was dried at 150oC for 20 h. Subsequently, this dried gel was subjected to thermal treatment at 700oC (for 2 hours) and 1000oC (for 2 hours) in kenthal high temperature furnace. The dried material was crushed to obtain fine powder of magnisio ferrite.

Composite polymer electrolyte films (~100-300µm thickness) were prepared using solution cast technique. The poly (ethylene oxide) PEO (mw~6x105 ACROS organics) and salt NH4SCN (Rankem India, AR grade) were used for the synthesis of composite electrolyte. The sol gel developed Mg-Zn ferrite powder was dispersed stoichiometrically in PEO-NH4SCN solution (in double distilled water at 40oC)

and stirred for 10-15 hours continuously. This gelatinous polymeric solution was finally cast in polypropylene dish. This solution cast film was dried at 30oC in B.O.D. incubator for controlled evaporation followed by vacuum drying to obtain the solvent free standing films of NCPE.

Structural behavior of Mg-Zn ferrite and PEO-NH4SCN: Mg-Zn ferrite system were studied by X-ray diffractometer (Phillips X-Pert model) in the Bragg's angle range (2θ) 15-60o using Cu-Kα radiation (λ=1.542 oA). Mossbauer study of magnisio ferrite powder was carried out by PC based spectrometer having 1024 channel MCA cord operating in constant acceleration mode. The SEM image of the different composite electrolyte system was recorded with JEOL JXA-8100 EPMA instrument. The electrical characterization of the solid polymer composite electrolyte was carried out using impedance spectroscopy on the application of small a.c. signal (~20mV) across the sample cell with Pt-blocking electrodes. The complex impedance parameter were measured with impedance analyzer (HIOKI LCR Hi-tester, model 3522, Japan) in the frequency range 40 Hz-100 KHz. Dielectric relaxation behaviors were carried out by the impedance data.

Solid State batteries are fabricated by sandwiching the solid electrolyte (NCPE in present studies) between two electrodes (cathode & anode). Hence the battery or cells consist of three major components i.e. anode, electrolyte and cathode. A typically, solid state cell in which NCPEs is sandwiched between anode and cathode of different chemical potentials μ1 and μ2 respectively. The solid state rechargeable batteries are assembled by two step process. In the first step, anode and cathode powdered materials are pressed in a pelletizing die to obtain pellets of electrodes. Since the focus of present work is to develop a proton conducting rechargeable all solid state battery, in order to supply protons, Zn+ZnSO4.7H2O with stoichiometric ratio 3:1 was chosen as anode material. The anode materials (Zn power & ZnSO4.7H2O) were crushed in agate to form fine powder. Thereafter this mixture was subjected to pelletizing die at ~5Kbar pressure for 20-30 minutes. Similarly cathode composite material comprising of (graphite, solid electrolyte, and any intercalation material like V2O5, MnO2, PbO2, and TiS2 in stoichiometric ratio 2:2:5) were again crushed and mixture was pelletized following the similar procedure. Finally, the NCPE sample possessing optimum conductivity were sandwiched between anode and cathode pellets. The cells dimension were approximately (dia-1.76cm, thickness 1to1.2cm and the so designed estimated cells weighed 2-4gram.

III. RESULTS AND DISCUSSIONS

A. Characterization of Mg-Zn Ferrite Powder:

X-ray diffraction pattern of sol gel derived magnesium zinc ferrite (magnisio ferrite) is shown in figure-1(a). The main reflections from the planes are identified as (220), (311), (400), (422) and (511) confirm to the earlier report on magnisio ferrite [16-19]. Appearance of prominent reflection from (311), (400) plane and absence of impurities peaks ascertain the formation of spinal cubic structure with single phase. From the XRD pattern for (311) plane lattice parameter was 0.85 a/nm obtained as which again tallies with reported data [JCPDS No. 00-008-0234] and thereby ascertain formation of mixed spinal magnesium-zinc ferrite. The relative concentration of Mg and Zn in ferrite structure is known to influence particle size and lattice parameter. The average particle size of the Magnisio ferrite powder was evaluated by the Scherer's formula and it is found to ~ 30 nm. Such a value suggests formation of nanoferrite.

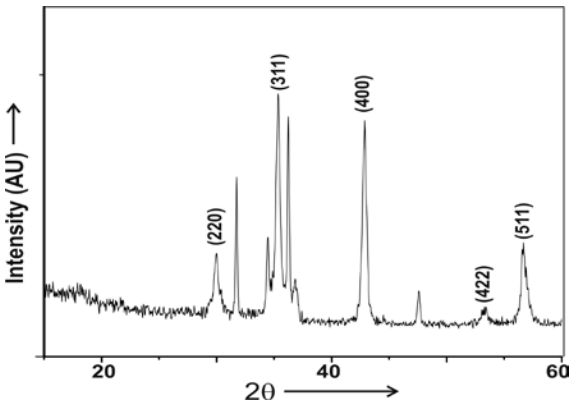

Figure 1 (a): XRD pattern of sol gel synthesized Mg-Zn ferrite powder.

RT.

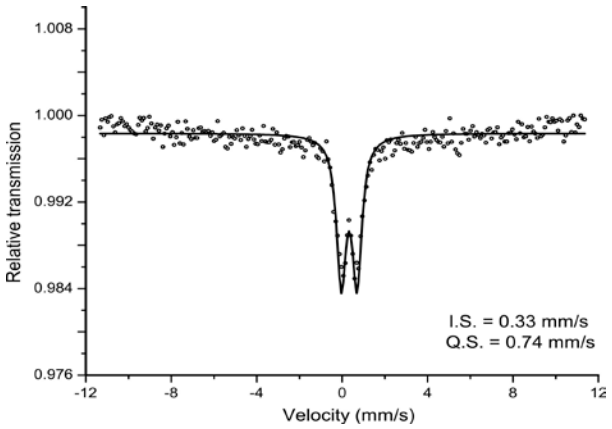

Figure 1 (b) Mossbauer Spectrum of nanosize Mg-Zn ferrite powder

Magnetic nano particle undergoing super paramagnetic relaxation is usually characterized by one of the powerful experimental technique namely, Mossbauer spectroscopy. At room temperature, in Mossbauer Spectrum the behavior of magnetic nano particles is quite interesting as they exhibit sextet (ferromagnetic state) and a doublet (super paramagnetic state). In Mossbauer Spectrum of Mg-Zn ferrite powder {shown in figure-1(b)} sample, the important observation is the appearance of a central doublet, related to absorption of quadrupole splitting. The spectra did not reveals any sextet. Careful examination of central doublet showed slight asymmetry to allow their assignment to presence of Fe3+ and Fe2+. The origin of central doublet components assigned to the Fe3+ ions and Fe2+ comes from super paramagnetic relaxation [20]. Further low value of isomer shift (IS~ 0.33mm/sec) and high value of quadrupole splitting (QS~ 0.74mm/sec) is attributed to small particle size (~nm) undergoing superparamagnetic relaxation at RT. Where, relaxation time τ is << τs (τs ~ characteristic time above blocking temperature). IS value of 0.33 mm/sec confirms only

the presence of Fe3+ was in ferrite sample while large Qs value indicates substantial electric field gradient around 57Fe nuclei due to small particle size.

B. Characterization of [93PEO-7NH4SCN]: x% Mg-Zn Ferrite Nanocomposite Polymer Electrolyte:

Structural behavior of [93PEO-7 NH4SCN]: x% Mg-Zn ferrite (where x= 0.5, 1, 2, 3, 4 and 5) system has been studied by XRD and SEM technique. The X-ray diffraction pattern of the different composite electrolyte system is shown in figure-2. In XRD pattern two main peaks at 19o and 23o (PEO characteristic peaks) with few other weak reflections are observed. Addition of salt and filler in polymeric host changes the intensity and broadness of existing original peaks. The increase in broadness or reduction in intensity is an indication of change (decrease) in crystallinity of pristine electrolyte. A comparative study of XRD peak at 23o shows splitting and broadening of the peak, with increase of filler content along with reduction in peak intensity. This reveals interaction of polymeric chain with salt and filler. The enlarged view of this interaction is also given in the inset of fig.-2 where we recorded few new peaks of Zn-Fe (2θ = 21.1o), Fe2O3 (2θ = 23.1o), Fe-Zn-CN (2θ = 23.3o), Zn (SCN)2 (2θ = 23.4o) and Fe-Zn(CN)6.2H2O (2θ = 23.5o). Existence of these peaks clearly supports interaction of PEO with NH4SCN and Magnisio ferrite. The average size of crystallites was calculated by the well known Scherer's formula [21].

$$t=0.9\lambda B\cos\theta \quad (1)$$

Where λ is the X-ray wavelength, θ the angle of Bragg's diffraction and B full width at half maximum (FWHM). The evaluated average crystallite sizes for different electrolytes were found to be 30-60 nm. In order to distinguish the effect of crystallite size induced broadening in FWHM of X-ray diffraction profile, Williamson-Hall (W-H) plot method [22] was adopted. In this method, crystallite size (without strain) is calculated from Sinθ vs. βCosθ plot {shown in figure-3} in accordance with the following relation.

$$\beta\cos\theta=C\lambda/t+2\varepsilon\sin\theta \quad (2)$$

Where C is the correction factor, ε the strain and λ, β and t have their usual meaning. The crystallite size (without strain) for different composite electrolyte system calculated by W-H plot method is given in table-1. These values ascertains nanometric dimension of synthesized electrolyte system.

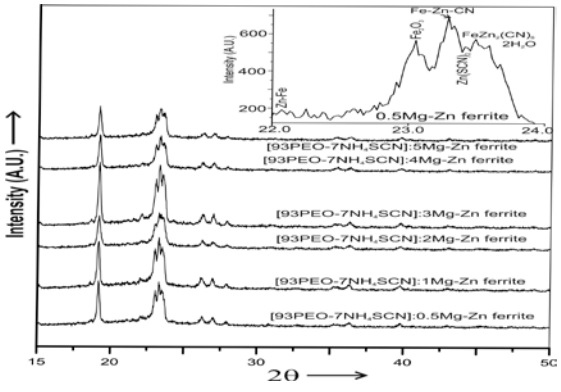

Figure 2: XRD pattern of (93 PEO-7NH4SCN): x% Mg-Zn ferrite film (where x = 0.5,1,2,3,4, 5). Enlarged view of the peak at 23° is given in inset.

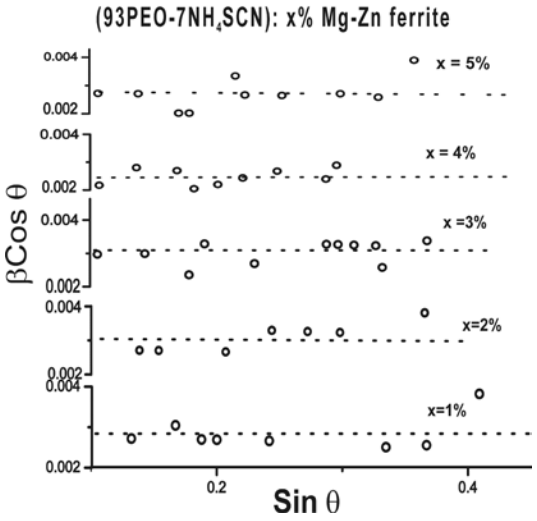

Figure 3: Williamson- Hall plots for different polymeric film.

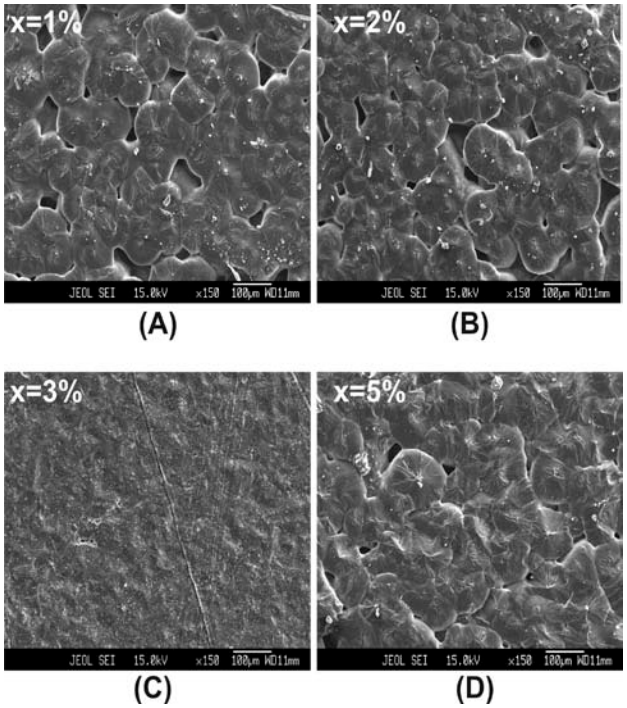

Figure 4: SEM image of (A) (93 PEO-7 NH4SCN):1% Mg-Zn ferrite film, (B) (93 PEO-7NH4SCN):2% Mg-Zn ferrite film, (C) (93 PEO-7 NH4SCN):3% Mg-Zn ferrite film and (D) (93 PEO-7 NH4SCN):5% Mg-Zn ferrite film.

SEM image of different compositions of [93PEO-7NH4SCN]: x% Mg-Zn ferrite (where x= 1, 2, 3 and 5 wt %) is given in figure-4. The images give the surface morphology and heterogeneous phase of nanocomposite electrolyte system. Pure PEO film has partial crystalline structure with formation of lamellar structure due to longer evaporation time used for drying the electrolyte films. Addition of Mg-Zn ferrite filler in [93PEO-7NH4SCN] electrolyte system make original entity looses this characteristic. Scanning electron images show that addition of filler disturbs the crystalline nature of original matrix. The particle size dimension during SEM analysis also supports the result of XRD studies.

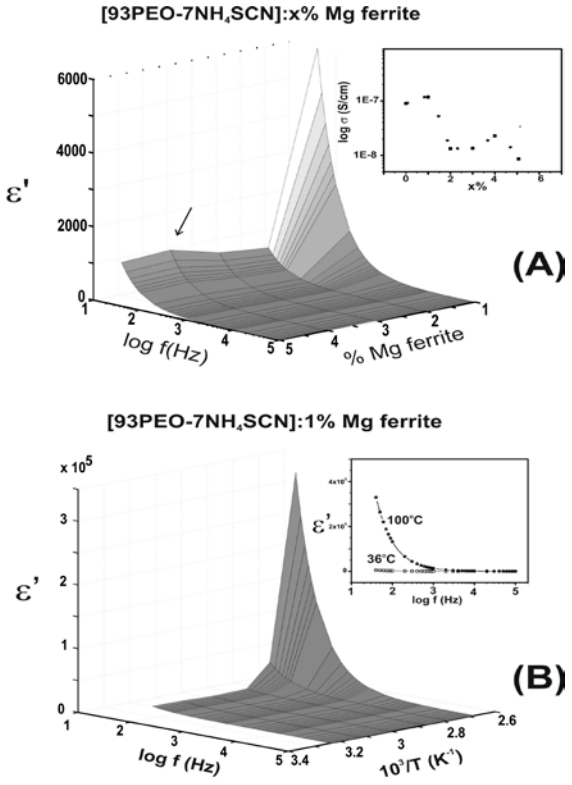

Figure 5 (a): Variation of Dielectric constant with frequency for different filler concentration (in inset Composition dependence of conductivity for polymer electrolyte system). (b): Variation of Dielectric constant with frequency and temperature for (93 PEO-7 NH4SCN):1% Mg-Zn ferrite film.

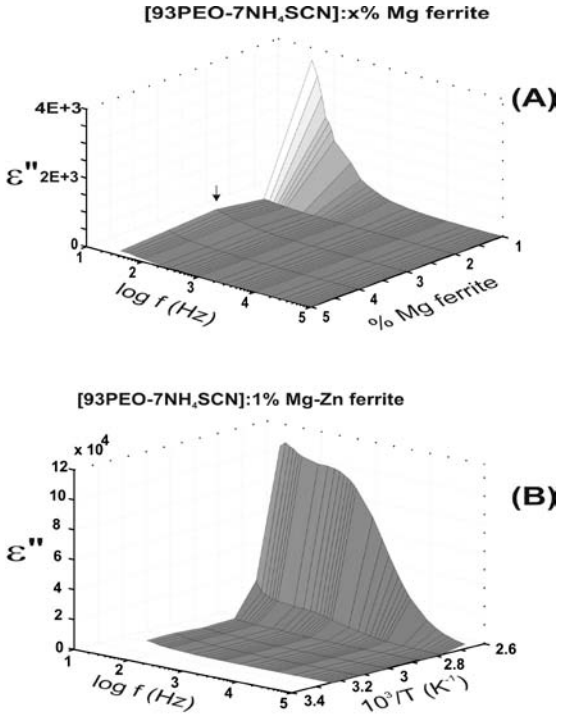

Figure 6 (a): Variation of imaginary part of Dielectric relaxation with frequency for different filler concentration. (b): Variation of imaginary part of Dielectric relaxation with frequency and temperature for){ 93 PEO-7 NH4SCN}:1% Mg-Zn ferrite film.

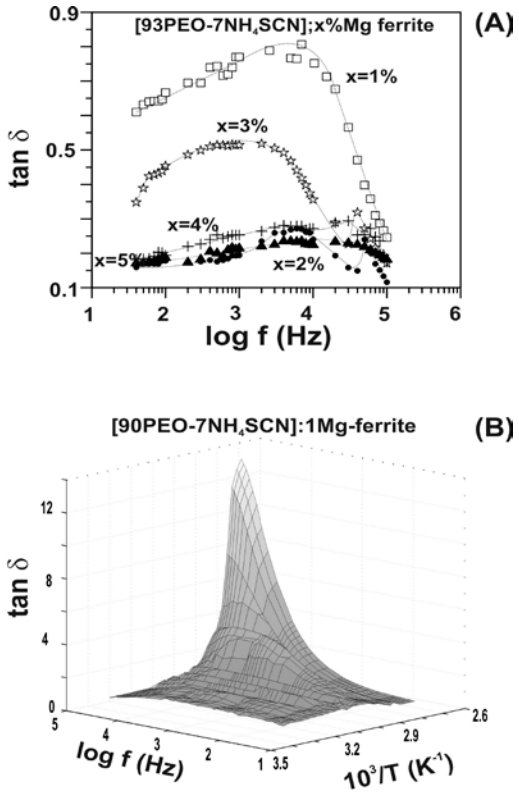

Figure 7 (a): Variation of Dielectric tangent loss with frequency for different filler concentration. (b): Variation of Dielectric tangent loss with frequency and temperature for {93 PEO-7 NH4SCN}:1% Mg-Zn ferrite film.

The change in relative dielectric constant of composite polymer electrolyte with frequency and Magnisio ferrite concentration is given in figure-5(a). Concentration dependence of ε′ shows two maxima: one at 1% Magnisio ferrite and the other at 4% magnisio ferrite concentration analogous to conductivity behavior. The change in bulk electrical conductivity with the ferrite composition is also given in the inset of figure-5(A) for comparison. Further strong frequency dispersion in relative permittivity (ε′) were recorded in low frequency region followed by a nearly frequency independent nature at higher frequencies above 10 KHz. Such a feature is typical of polymeric substance [23]. The decrease of ε′ with increasing frequency may be attributed to electrical relaxation or inability of dipoles to rotate rapidly leading to a lag between frequency of oscillating dipoles and that of applied field. As the frequency increases the ionic and orientational source of polarizibility decreases and finally disappears due to inertia of mobile ions which causes a constant value of dielectric constant [24]. This is possibly due to suppression of large scale heterogeneity in pristine complex and its replacements by small scale heterogeneity. The small scale heterogeneity is related to presence of Mg-Zn ferrite filler which increases the free volume on account of looser segmental packing of chain [25]. The frequency dependence of the dielectric constant on composition of electrolyte is explained as the polarizibility and potential movement of ions. In polymer host PEO, the oxygen ion is the mostly polarizable ion. Thus frequency dependent dielectric relaxation below 1 KHz could be related to ionic space charge carriers, such as oxygen vacancies, anti

site defects and interfacial polarization. Interaction of Mg-Zn ferrite with salt and polymer has been witnessed during XRD studied. This leads to formation of most easily polarizable non bridging oxygen. This enhances the dielectric constant of the composite system. The observed two maxima in dielectric constant can be associated to interfacial polarization followed by polarization resulting from polymer-salt- filler interaction. At high filler content i.e. beyond 1 wt% ferrite filler in electrolyte decrease the dielectric polarization comes from increase in crystalline behavior. A moderate rise in dielectric constant around 4 wt% filler content may be possibly due to the increase in polarizibility of polymer in the presence of ferrite. When the filler content is enhanced further its segregation takes place which reduces the polarizibility of composite system.

The variation of dielectric constant of [93PEO-7NH4SCN]: 1% Mg-Zn ferrite nanocomposite electrolyte system (maximum conductivity system) with frequency and temperature is given in figure 5(b). A strong dielectric dispersion was observed with increasing temperature. It is interesting to note that the non Debye nature of electrolyte system at low temperature and low frequency value was recorded while it continued to high temperature for higher frequency value. The observed behavior can be explained if the system is assumed to be formed of molecular dipoles. These dipoles remain frozen when the temperature is lower than (345oK). As the temperature increase beyond this critical temperature (Tc), the dipoles becomes more thermally activated having more rotational freedom, which leads to the observed increase in the dielectric relaxation.

The change in imaginary part of dielectric permittivity (or dielectric loss) with frequency and Mg-Zn ferrite concentration is shown in figure 6(a). The dielectric study gives two maxima for dielectric loss with variation of Mg-Zn ferrite content in consonance with dielectric constant variations. The value of ε″ is seen to decrease with increasing frequency at room temperature- a well known feature seen in polymer electrolytes [26]. Higher value of dielectric loss (ε″) at low frequency is due to the free charge motion within electrolyte. It also reflects the reorientation process of dipoles in polymer chain which gives a relaxation peak in dielectric loss spectra.

The Figure- 6(b) shows the variation of dielectric loss/ imaginary part of dielectric permittivity with frequency and temperature. The dielectric loss is noticed to increase with increasing temperature of [93PEO-7NH4SCN]: 1% Mg-Zn ferrite system. It is possibly due to formation of extra molecular dipoles in the system. These dipoles become thermally activated, having more rotational freedom. It is thus inferred that all types of polarization except for thermally activated space charge polarization may contributing to the dielectric polarization response in the low temperature range. On other hand, at higher temperature beyond melting temperature of polymer host, the thermally activated space charge may be contributing to polarization process, which leads to observed increase in ε″ and the dispersion process. The entire response reflects a non-Debye relaxation in composite electrolyte system.

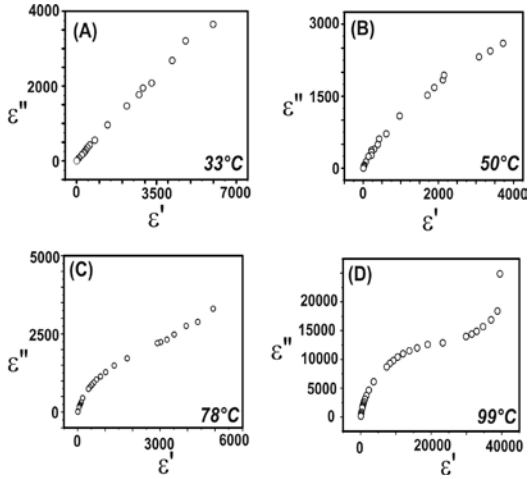

Figure 8 Cole- Cole plot for dielectric relaxation at different temperature for (93 PEO-7 NH4SCN):1% Mg-Zn ferrite film.

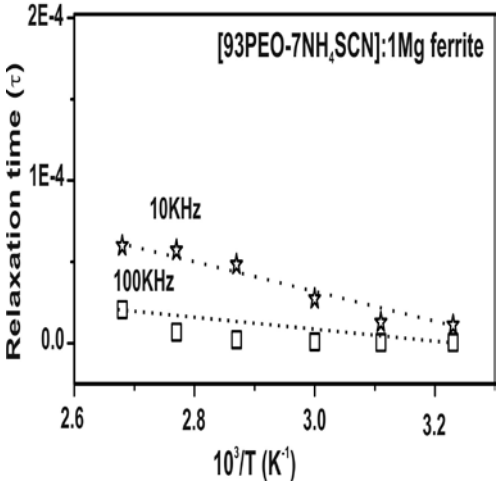

Figure 9 Variation of relaxation time with temperature for (93 PEO-7 NH4SCN):1% Mg-Zn ferrite film.

The frequency dependence of dielectric tangent loss (tanδ), at different compositions is shown in figure-7(a). The composition dependent curve of tangent loss shows a clear relaxation peak with increase in its broadness with the rise of Mg-Zn ferrite content, in composite system. And it was tend to decrease the peak frequency for relaxation. Also loss tangent value decreases significantly with increasing ferrite concentration (up to 2wt %) and thereafter it increases, before finally decreasing due to segregation of filler in polymer chain. This nature is also a reflection of two peaks characteristics of the system. The loss peak can be successfully explained in term of the dielectric relaxation process associated with the presence of crystal heterogeneity in the polymer electrolyte matrix [27]. All these results show that enhancement of Mg-Zn ferrite content tend to looses the segmental packing in the chain thereby increasing the free volume for dipolar relaxation. XRD studies shows that addition of filler enhances the amorphousity of the polymer electrolyte film up to a certain limit. This peak can be attributed to segmental diffusion motion in amorphous region and assignable to β (beta) relaxation process.

TABLE-1: AVERAGE PARTICLE SIZE FOR DIFFERENT POLYMER COMPOSITE ELECTROLYTES.

S No Sample	particle size by Scherer's formula(nm)	particle size by W.H Plot(nm)
1. $Mg_{1-x}Zn_xFe_2O_3$(Magn is io ferrite)	29.5	22.5
2. [93PEO-7NH $_4$SCN]:0.5% Mg -Zn ferrite	47.2	43.5
3 . [93PEO-7NH $_4$SCN]:1% Mg -Zn ferrite	45.8	31.0
4 . [93PEO-7NH $_4$SCN]:2% Mg -Zn	38	35
5 . [93PEO-7NH $_4$SCN]:3% Mg -Zn	57	45
6 . [93PEO-7NH $_4$SCN]:4% Mg –Zn	35	32
7 . [93PEO-7NH $_4$SCN]:5% Mg -Zn ferrite	59	52

The variation of tangent loss with frequency and temperature is shown in figure -7(b). From the curve it can be noted that, as the frequency increases the peak maxima tend to shift to higher temperature, indicating the temperature dependence of the relaxation time. Presence of relaxation dipoles may be due to the orientation of the polar groups present in the side group of the polymer. This type of relaxation is called the dipolar group relaxation.

The dielectric behavior for the polymeric material can be described by the Cole-Cole expression [28, 29].

$$\varepsilon^* = \varepsilon_\infty + \Delta\varepsilon(1+i\omega\tau)^y \quad (3)$$

Where ε∗ is complex dielectric constant, $\Delta\varepsilon = \varepsilon - \varepsilon\infty$ the static dielectric constant, ε∞ the relative dielectric constant at very high frequency, τ the effective relaxation time, y a parameter (defined as angle of semicircular arc) where value lies in the range $0 < y < 1$ to describe the distribution of relaxation time and $\omega = 2\pi f$ is the angular frequency. When y =1 the equation gives semicircle (cole-cole plot) in the plot of ε″ verses ε′ and reduced to the non cooperative single relaxation following in the linear Arrhenius relation [30]. The variation of ε″ (imaginary part) versus ε′ (real part) i.e. cole-cole plot is shown in figure-8. In the Cole-Cole plot the decrease in diameter of semicircle is observed with increase in temperature.

Based on equation (3), the relaxation frequency of dielectric absorption f max is expressed as

$$2\pi f_{max} = \tau \quad (4)$$

Where the dispersion and absorption curves are symmetrical about the position $\omega\tau = 1$. The relaxation time τ is determined by experimentally obtained frequency fmax. The calculated relaxation time for this system is ~ 8.5x10-5 sec. Figure-9 shows the variation of relaxation time (τ) against reciprocal of absolute temperature. The relaxation time linearly increases with temperature. This gives Arrhenious type thermally activated process. The slope yield activation energy for dielectric relaxation process.

For the study of electrode polarization/interfacial polarization effect in the nanocomposite electrolyte system as mentioned earlier the dielectric spectra and its scaling by complex modulus electric spectra was carried out [31].

The complex modulus can be evaluated from the following relation

$$M = M' - j\,M''$$

$$M' = \varepsilon''/\{(\varepsilon'')^2 + (\varepsilon')^2\} \text{ and } M'' = \varepsilon'/\{(\varepsilon'')^2 + (\varepsilon')^2\} \quad (5)$$

Figure -10 shows the real and imaginary part of dielectric modulus with frequency at different temperature (36-100oC) for [93PEO-7NH4SCN]: 1% Mg-Zn ferrite nanocomposite electrolyte system. The real part of modulus spectra increases with increasing frequency and decreases with increasing temperature. Also the imaginary part of dielectric modulus spectra increases with increasing temperature and frequency. In this case, electrode polarization / interfacial polarization effect is seen to completely vanish in contrast to the dielectric formalism. This is observed around frequencies (<500Hz). The appearance of peak in imaginary part of the dielectric modulus can be assumed to be related with the translation ionic dynamics and the conductivity relaxation of the mobile ions. We have also examined the scaling behaviour of the modulus function. M' and M" spectra scaled by M"max and frequency axis scaled by the relaxation frequency f max are shown in figure -10(b) and (d) for [93PEO-7NH4SCN]: 1% Mg-Zn ferrite nanocomposite electrolyte system.

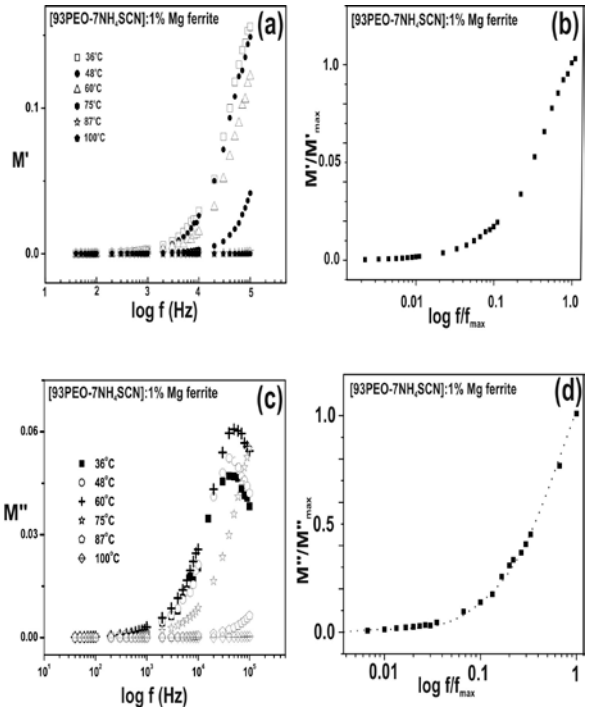

Figure 10: Variation of (a) Real part of electric modulus (M') with frequency at different temperature (b) Normalize M' with normalize frequency (c) Imaginary part of electric modulus (M") with frequency at different temperature and (d) Normalize M" with normalize frequency.

The variation of a. c. conductivity with different filler concentration in [93PEO-7NH4SCN]: x% Mg-Zn ferrite nanocomposite electrolytes system are given in figure- 11(a). The a. c. conductivity of 1% Mg-Zn ferrite filler content remains same with increasing the frequency, but for higher ratio of ferrite a. c. conductivity decreases with ferrite content. For other compositions i.e. for [93PEO-7NH4SCN]: x% Mg-Zn ferrite (x= 2, 3, 4, & 5%), the conductivity increases monotonically with frequency and beyond 10 KHz it rapidly grows (to form a peak). The frequency dependent conductivity in solid polymer electrolyte system seems to follow Universal power law [32].

TABLE-2 BATTERIES PARAMETERS OF NANO COMPOSITE POLYMER ELECTROLYTES

Solid State rechargeable battery parameters	OCV (Volt)	Current (I) (μA)	Electric Power (P) (μW)	Electric energy (E) (μWh)	Current density (J) (μAcm^{-2})	Power density (μW/Kg)	Energy density (μWh/Kg)
[93PEO-7NH_4SCN]:1% Mg-Zn ferrite	1.57	1.4	1.69	2.53	0.71	670	1003

$$\sigma_{ac}=\sigma_o+A\omega^n \quad (6)$$

Where, σo is the dc conductivity (extrapolation of the platue region to zero frequency gives the d. c. ionic conductivity), A the pre-exponential factor and n the fraction exponent laying between 0&1. The calculated value of conductivity for the best conducting electrolyte i.e. [93PEO-7NH4SCN]: 1% Mg-Zn ferrite composition is σo = 9.0x10-5 S/cm, and n=1. The change in a. c. conductivity is not prominently observed with applied frequency. This means that the charge carriers are not sufficiently free to follow the changing electric field and therefore conductivity remains nearly frequency independent. Figure -11(b) shows the variation of a. c. conductivity against frequency and temperature for [93PEO-7NH4SCN]: 1% Mg-Zn ferrite. In NCPEs a.c., conductivity increases linearly with frequency and temperature.

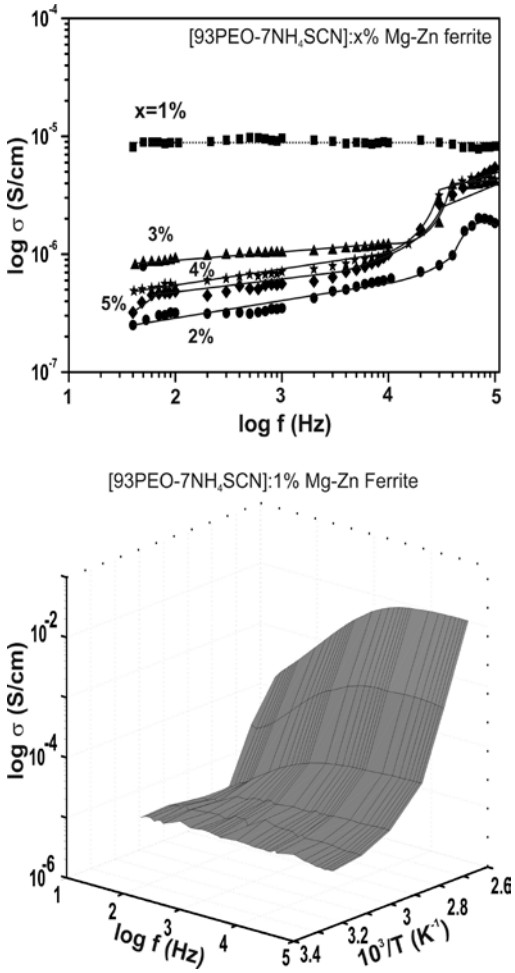

Figure 11 (a): Variation of ac conductivity with frequency for different composition of nano polymer composite electrolytes at ambient temperature. (b):Variation of ac conductivity with frequency for [93PEO-7 NH4SCN]: 1% Mg-Zn ferrite at different temperature.

In order to study the physical mechanism of the induced dielectric constant, the frequency dependence of the dielectric constant (ε'), imaginary part of dielectric permittivity (ε″) and a.c. conductivity at room temperature were plotted as figure-12. Dielectric constant (ε') exhibits asymptotic drop with increasing frequency. Further the slope of ε″ vs. frequency is found to be near (-1) in low frequency range. The dielectric loss tanδ (as given in fig-8) mainly consists of two contributions one from the dielectric polarization process $\tan\delta_{relax.}$ and other from d.c. conduction $\tan\delta_{dc}$. So $\tan\delta_{ac}$ can be expressed as,

$$\tan\delta_{ac}=\sigma_{dc}\omega\varepsilon \quad (7)$$

Where $\omega = 2\pi f$ equation (7) can be rewritten as $\varepsilon''_{dc}= \sigma_{dc}/\omega$. This means that the slope of log ε''_{dc} vs log ω (or log f) is -1. This slope (-1) indicates that the predominant dc contribution in the studied nanocomposite polymer electrolyte system [33, 34].

Once of the basic requirements of these entire polymer electrolytes is high ionic conductivity over a wide temperature window to establish their worth in electrochemical devices. Thus, besides structural, thermal and electrochemical characterizations, electrical characterization of NCPE is yet another important factor. Keeping this in mind electrical characterization on the developed nanocomposite polymer electrolytes was pursued.

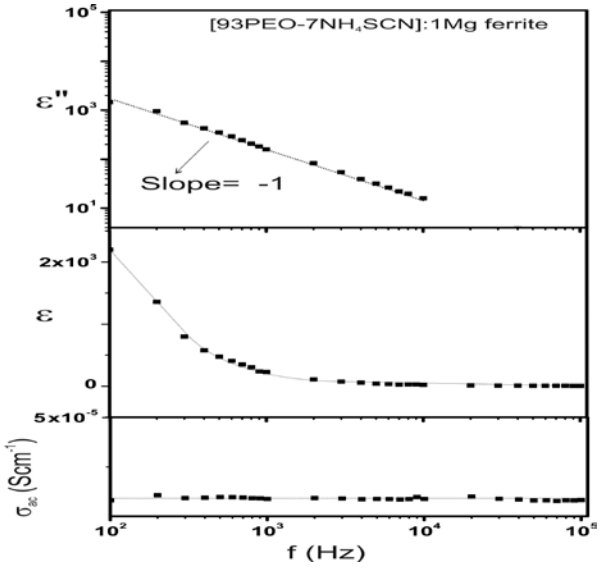

Figure 12: Frequency dependence of the ε', ε" and ac conductivity for[93PEO-7NH4SCN]: 1% Mg-Zn ferrite system.

The performance of a battery is evaluated from the cell parameters [35-37]. Various related parameters on the batteries based on NCPE were estimated. The open circuit voltage (OCV) of fabricated were noted using high resolution multimeter and were found to be 1.57 V of Mg-Zn ferrite

doped NCPE for [93PEO-7NH_4SCN]: 1% Mg-Zn ferrite. After OCV measurements these cells were subjected to self discharge without any application of load for long time and these cells were charged again on the application with constant current and 3V potential. The charge discharge characteristics were recorded on different load conditions. These parameters were calculated using following relations [38].

1) Electric Power (P):

This is the product of cell voltage (V) and current (I) delivered to the external load of resistance (R)

$$P = V.I = I^2R = V^2/R \text{ [W]}$$

2) Electric Energy (E):

This is the product of power and the discharge time in hour

$$E = V.I.t = q.\ V \quad \text{[Wh]}$$

3) Energy Density (Volume Capacity):

This is defined as the ratio of electric energy (E) and battery volume (v) in

$$E.D. = E/v \quad \text{[Wh/cc]}$$

4) Specific Energy (Weight Capacity):

This is the ratio of electric energy (E) and battery weight (m)

$$S.E. = E/m \quad \text{[Wh/Kg]}$$

5) Specific Power (Power Density):

This is defined as the ratio of electric power (P) and battery weight (m) in

$$P.D.= P/m \quad \text{[W/Kg]}$$

6) Current Density (J)

It is the defined as of current (I) and area of the cell

$$J = I/A \quad [A/cm^2]$$

All the fabricated cells were found to run for more than 200h at low current drain (1.5μA/cm^2). Further, the cell can withstand 10-20 cycles making it suitable low current density applications. All these parameters were determined in the plateau region of the cell potential discharge profile by 1MΩ resistance and values have been listed in table-2.

IV. CONCLUSIONS

The experimental studies through XRD, SEM, dielectric relaxation and electrical conductivity show that the Mg-Zn ferrite nano-filler changes the physical and morphological behavior of nano-composite electrolyte. Mossbauer investigations reveal the superparamagnetic nature of the Magnisio ferrite powder. XRD and SEM observations confirm formation of nano-composite system with crystallite size varying in between 30-60 nm. The electrical conductivity is enhanced by ~3-4 orders upon dispersion of ferrite and which also controls the gap of crystalline and amorphous conductivity. OCV of proton conducting battery were found to be 1.57 Volt.

ACKNOWLEDGMENT:

Thanks to BRNS, Dept. of Atomic energy Govt. of India for the financial support (No. 2009/34/25/BNRS) for this work.

REFERENCES

[1] Owen J. R , Superionic solids and solid electrolytes recent trends, 1989, In: Laskar A.L., Chandra S. ed. Academic Press, 111.

[2] Agrawal R. C., Pandey G. P. 2008 J Phys. D: App. Phys.41 223001.

[3] Koo J.H., Polymer nanocomposites: processing, characterization, andapplications, 2006 McGraw-Hill Professional 79.

[4] Pandey K., Dwivedi M. M., Tripathi M., Singh M. and Agrawal S.L 2008 Ionics 14 515.

[5] Maccallum J. R., Vincent C.A. 1987 Polymer Electrolyte Reviews, Elsevier. Applied Science.

[6] Chandra A., Srivastava P. C., Chandra S. 1995 J. Mater. Sci. 30 3633.

[7] Awadhia A., Patel, S.K., Agrawal S.L. 2006 Progress in Crystal Growth and Characterization of Materials 52 61.

[8] Alamgir, M., Abraham, K.M. 1993 J .Electrochem. Soc. 140 L96.

[9] Rajendran S., Uma T., 2000 Mater. Lett. 44 208.

[10] Tsuchida H., Toko T., 1983 Jpn. J. Appl. Phys. 22 1543.

[11] Bohnke O. and Vuillemin B., 1992 Mater. Sci. Eng. B 12 243.

[12] Appetechi G.B., Croce F., Scrosati B., 1995 Electrochim. Acta 40 991.

[13] Tanwar A., Gupta K.K., Singh J.P., Vijai Y.K., 2006 Bull. Mater. Sci. 29 397

[14] Pandey K., Dwivedi M. M., Singh M., Agrawal S. L., 2010 Journal of Polymer Research, 17 127.

[15] Iyer R., Desai R. Upadhyay R.V., 2009 Bull. Mater. Sci. 32 141.

[16] Rittidech A., Porkornwong N., Suthapintu A., 2009 Ferroelectrics, 382 62.

[17] Bharathi Kannan R., Chandramohan A., Chandra Sekar J., Kandhaswamy M. A., 2007 Crystal Research and Technology, 42 595.

[18] Mazen S.A., Mansour S.F., Zaki H.M., 2003 Cryst. Res. Technol., 38 471.

[19] Bammannavar B.K., Naik L.R., Pujar R.B., Chougule B.K., 2007 Indian J. Engg. & Mater. Sci. 14 381.

[20] Nath B.K., Chakrabarti P.K., Das S., Kumar U., Mukhopadhyay P.K., Das D. 2005 J. Surface Sci. Technol., 21 169.

[21] Cullity B.D. 1978 Element of X-ray diffractinon, Anderson-Wesley, 2nd ed. 281

[22] Williamson G.K., Hall W.H. 1953 Acta Metall. 1 22.

[23] León C., Lucía M. L., Santamaría 1997 J., Physical Review B 55 882.

[24] Pradhan D.K., Choudhary R.N.P., Samantaray B.K. 2008 Int.J. Electrochem.Sci., 3 597.

[25] Waser R., Baiatu T., Hardtl K.-H., dc electrical degradation of perovskite-type titanates: I ceramics, 1990 J. Amer. Ceram. Soc.73 1645.

[26] Pandey K., Dwivedi M. M., Das I.M.L., Singh M., Agrawal S. L. 2010 Journal of Electroceramics, 25 99.

[27] Marzantowicz M., Dygas J. R., Krok F., Florjanczyk Z., Zygadlo-Monikowska E., 2006 J. Non-Crystalline Solids, 352 5216.

[28] Kundu R.S., Bhatia K.L., Kishor N., Jain V. 1996 Philos. Mag.B. 74 317.

[29] Chaudhari B.K., Chaudhari K., Som K.K., 1989 J. Phys. Chem. Solid, 50 1149.

[30] Blythe A.R.1977 Electrical Properties of Polymers, Cambridge University Press.

[31] Moynihan C.T., Boesch L.P. Laberge N.L.1973 Phys. Chem. Glasses 14 122.

[32] Jonscher A.K. 1983 Dielectric Relaxation in Solids, London: Chelsea Dielectric Press.

[33] Chen A., Zhi Y. 2000 Phys. Rev. B 61 11363.

[34] Chen A., Zhi Y., Cross L.E., Guo R., Bhalla S.A. 2001 Appl. Phys. Lett. 79 818.

[35] Scheers J., Johansson P., Szczecinski P., Wieczorek W.,Armand M., Jacobsson P., Scheers J., Johansson P., 2010 Journal of Power Sources 195 6081.

[36] Syzdeka J., Armand Michel, Gizowskaa M., Marcinek M., Sasima E., Szafran M., Wieczorek W. 2009 Journal of Power Sources 194 66.

[37] Pandey K., Laksmi N., Chanrda S. 1998 Journal of Power Sources 76 116.

[38] Julien C., Nazri G.A.1994.Solid State Batteries: materials Design and Optimization, Kluwer Academic Publishers, London,